

Analysis of the electrostatics in Dy^{III} single-molecule magnet: the case study of Dy(Murex)₃

J. Jung,^a X. Yi,^b G. Huang,^b G. Calvez,^b C. Daiguebonne,^b O. Guillou,^b O. Cador,^c A. Caneschi,^d T. Roisnel,^a B. Le Guennic^{a*} and K. Bernot^{b*}

SUPPLEMENTARY INFORMATION

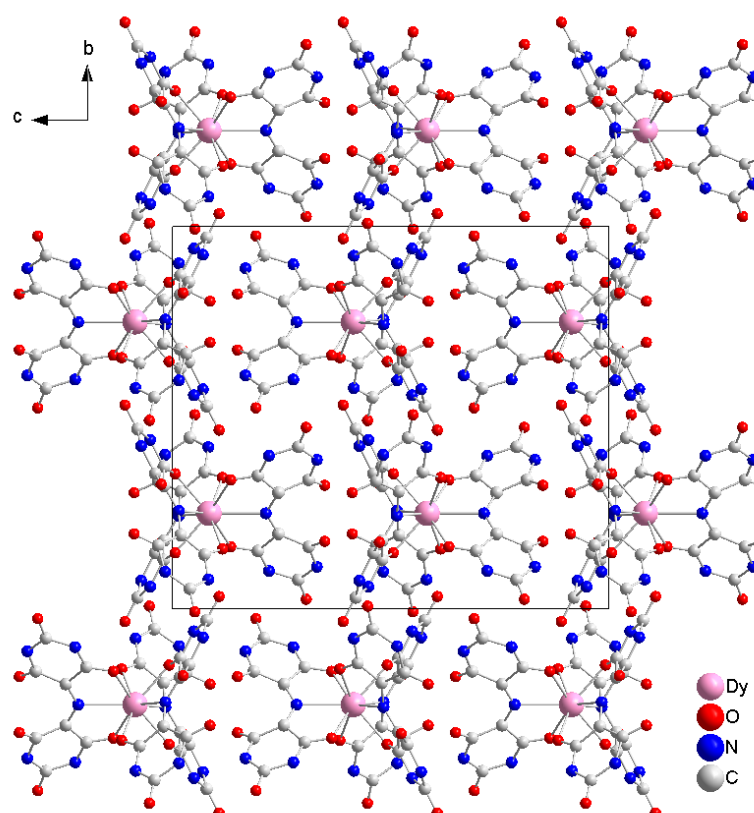


Figure S1. View of the crystal packing of **1** along the *a* axis (H atoms, water molecules and complexes from neighbouring cell omitted for clarity).

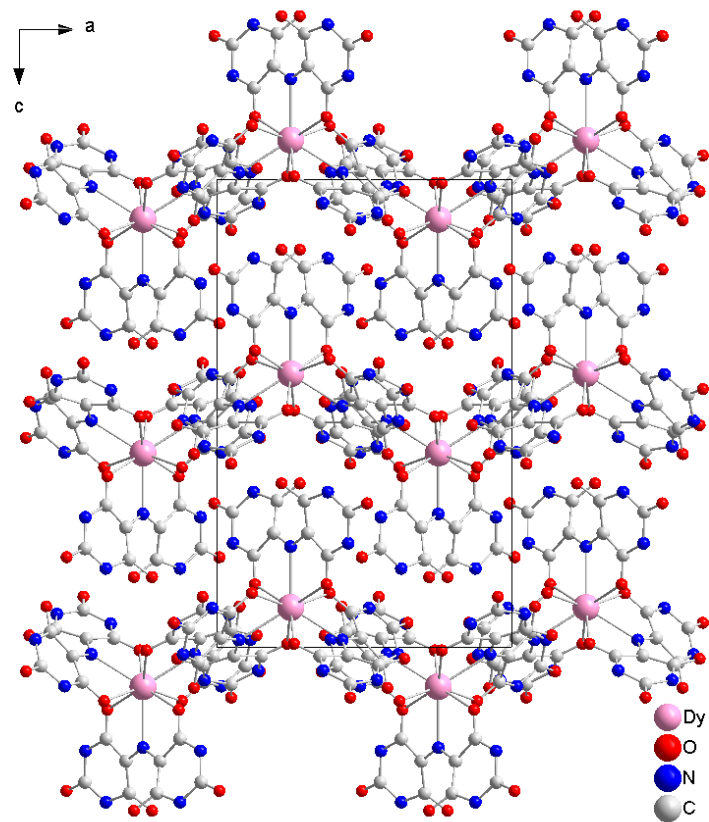


Figure S2. View of the crystal packing of **1** along the **b** axis (H atoms, water molecules and complexes from neighbouring cell omitted for clarity).

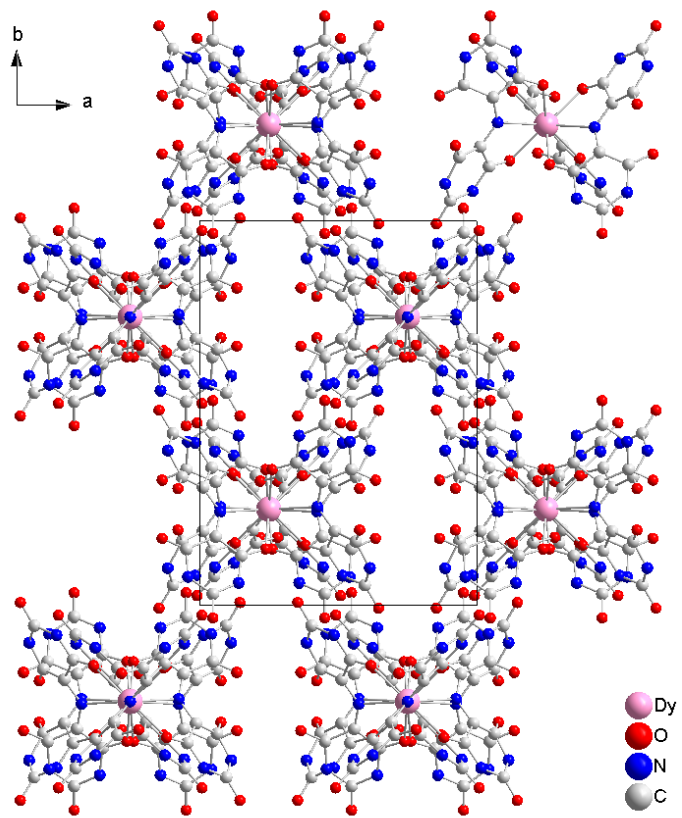


Figure S3. View of the crystal packing of **1** along the *c* axis (H atoms, water molecules and complexes from neighbouring cell omitted for clarity).

Table S1. Main crystallographic parameters.

Compound	1
CCDC number	1409034
Formula	C24 H12 Dy N15 O18
M / g.mol ⁻¹	960.99
Crystal system	Orthorhombic
Space group	P c c n
Cell parameters	12.4420(2) 17.2570(3) 19.7040(5)
Volume / Å ³	4230.68(17)
Cell formula units	4
T / K	150
λ (Å)	0.71073
Θ range	2.03-27.50
Number of reflections	20045
Independent reflections	4848
Fo > 4σ Fo)	3140
Number of variables	263
μ	1.850
Highest difference peak Largest diff. peak and hole	0.797 and -1.63 e.Å ⁻³
Goof, R ₁ , wR ₂	1.073, 0.0406, 0.1532

$$R_{int} = \frac{\sum |F_o^2 - \langle F_o^2 \rangle|}{\sum F_o^2}$$

$$S = \left\{ \frac{\sum [w(F_o^2 - F_c^2)^2]}{n-p} \right\}^2$$

$$R_1 = \frac{\sum |F_o| - |F_c|}{\sum F_o}$$

$$wR_2 = \left\{ \frac{\sum [w(F_o^2 - F_c^2)^2]}{\sum [w(F_o^2)^2]} \right\}^{1/2}$$

$$w = 1 / \left[\sigma(F_o^2) + (aP)^2 + bP \right]$$

$$\text{with } P = \left[2F_c^2 + \text{Max}(F_o^2, 0) \right] / 3$$

Table S2. Selected bond lengths (Å).

	bond lengths (Å)
Dy1-O6	2.344(4)
Dy1-O2	2.356(4)
Dy1-O5	2.375(4)
Dy1-N7	2.573(5)
Dy1-N8	2.570(7)
Dy1-Dy1	9.852(5)

Table S3. Selected angles (°).

Atom 1	Symmetry 1	Atom 2	Symmetry 2	Atom 3	Symmetry 3	Angle
O6	x, y, z	Dy1	x, y, z	O6	0.5-x, 0.5-y, z	130.71(19)
O6	x, y, z	Dy1	x, y, z	O2	0.5-x, 0.5-y, z	75.15(13)
O6	0.5-x, 0.5-y, z	Dy1	x, y, z	O2	0.5-x, 0.5-y, z	142.95(12)
O6	x, y, z	Dy1	x, y, z	O2	x, y, z	142.95(12)
O6	x, y, z	Dy1	x, y, z	O5	0.5-x, 0.5-y, z	83.50(14)
O6	0.5-x, 0.5-y, z	Dy1	x, y, z	O5	0.5-x, 0.5-y, z	84.30(14)
O6	0.5-x, 0.5-y, z	Dy1	x, y, z	O5	x, y, z	83.50(14)
O6	x, y, z	Dy1	x, y, z	O5	0.5-x, 0.5-y, z	83.50(14)
O5	0.5-x, 0.5-y, z	Dy1	x, y, z	O5	x, y, z	150.49(19)
O6	x, y, z	Dy1	x, y, z	N8	x, y, z	65.36(10)
O2	0.5-x, 0.5-y, z	Dy1	x, y, z	N8	x, y, z	130.53(9)
O2	x, y, z	Dy1	x, y, z	N8	x, y, z	130.53(9)
O5	0.5-x, 0.5-y, z	Dy1	x, y, z	N8	x, y, z	75.24(10)
O5	x, y, z	Dy1	x, y, z	N8	x, y, z	75.25(10)
O6	x, y, z	Dy1	x, y, z	N7	0.5-x, 0.5-y, z	69.60(13)
O6	0.5-x, 0.5-y, z	Dy1	x, y, z	N7	0.5-x, 0.5-y, z	142.42(13)
N8	x, y, z	Dy1	x, y, z	N7	x, y, z	122.16(10)
N7	0.5-x, 0.5-y, z	Dy1	x, y, z	N7	x, y, z	115.69(19)
O2	x, y, z	Dy1	x, y, z	N8	x, y, z	130.53(9)
O5	0.5-x, 0.5-y, z	Dy1	x, y, z	N8	x, y, z	75.24(10)
O5	x, y, z	Dy1	x, y, z	N8	x, y, z	75.25(10)

Table S4: Wave functions of the 16 spin-orbit states of the ground multiplet. States 1 and 2 correspond to the ground multiplet, states 3 and 4 to the first excited state and so on until the 8th Kramer doublet.

	1	2	3	4	5	6	7	8	9	10	11	12	13	14	16	
-15/2	0,83	0,00	0,08	0,00	0,17	0,00	0,00	0,10	0,03	0,32	0,01	0,35	0,00	0,22	0,00	0,05
-13/2	0,17	0,01	0,53	0,14	0,37	0,25	0,13	0,16	0,09	0,11	0,27	0,21	0,30	0,43	0,12	0,09
-11/2	0,02	0,03	0,18	0,08	0,56	0,10	0,42	0,03	0,03	0,42	0,31	0,17	0,35	0,09	0,14	0,08
-9/2	0,24	0,00	0,04	0,05	0,10	0,17	0,26	0,56	0,32	0,45	0,31	0,27	0,21	0,01	0,02	0,06
-7/2	0,43	0,01	0,20	0,08	0,20	0,21	0,07	0,44	0,15	0,17	0,02	0,51	0,09	0,37	0,08	0,17
-5/2	0,05	0,02	0,57	0,11	0,10	0,07	0,02	0,33	0,17	0,31	0,06	0,08	0,29	0,38	0,31	0,28
-3/2	0,18	0,07	0,24	0,15	0,41	0,23	0,14	0,17	0,08	0,39	0,01	0,08	0,32	0,13	0,43	0,38
-1/2	0,06	0,06	0,39	0,20	0,11	0,28	0,06	0,19	0,22	0,07	0,38	0,22	0,09	0,06	0,40	0,50
1/2	0,06	0,06	0,20	0,39	0,28	0,11	0,19	0,06	0,07	0,22	0,22	0,38	0,06	0,09	0,50	0,40
3/2	0,07	0,18	0,15	0,24	0,23	0,41	0,17	0,14	0,39	0,08	0,08	0,01	0,13	0,32	0,38	0,43
5/2	0,02	0,05	0,11	0,57	0,07	0,10	0,33	0,02	0,31	0,17	0,08	0,06	0,38	0,29	0,28	0,31
7/2	0,01	0,43	0,08	0,20	0,21	0,20	0,44	0,07	0,17	0,15	0,51	0,02	0,37	0,09	0,17	0,08
9/2	0,00	0,24	0,05	0,04	0,17	0,10	0,56	0,26	0,45	0,32	0,27	0,31	0,01	0,21	0,06	0,02
11/2	0,03	0,02	0,08	0,18	0,10	0,56	0,03	0,42	0,42	0,03	0,17	0,31	0,09	0,35	0,08	0,14
13/2	0,01	0,17	0,14	0,53	0,25	0,37	0,16	0,13	0,11	0,09	0,21	0,27	0,43	0,30	0,09	0,12
15/2	0,00	0,83	0,00	0,08	0,00	0,17	0,10	0,00	0,32	0,03	0,35	0,01	0,22	0,00	0,05	0,00

Table S5: Computed properties of Dy(Murex)₃ for the 8 first KD of the system: relative energy in cm⁻¹, magnetic anisotropy tensors and deviation angle between the main magnetic direction of the ground KD and all the other Kramer doublets.

# Spin-orbit state	Relative energy (cm ⁻¹)	Magnetic anisotropy tensor (g _x , g _y and g _z)	Deviation angle (°) with the main magnetic easy-axis of the ground state
1	0	0.20	
		0.27	
		16.58	
2	24	3.56	
		3.64	55
		13.26	
3	52	7.97	
		6.82	78
		2.47	
4	73	10.98	
		6.52	27
		0.52	
5	99	10.04	
		7.82	46
		1.03	
6	165	7.64	
		5.93	17
		3.59	
7	214	9.91	
		7.76	53
		2.32	
8	337	0.12	
		0.33	90
		18.78	

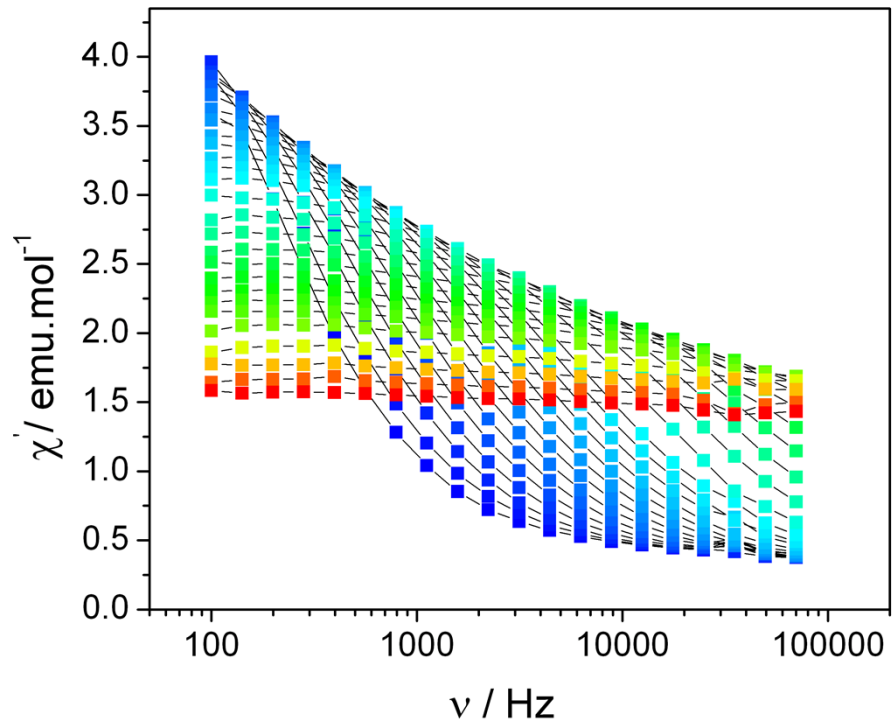


Figure S5. Frequency dependence of the out-of phase susceptibility (χ_M'') with temperature ranging from 1.7 (blue) to 7.1 K (red) measured with a 1500 Oe external dc field.

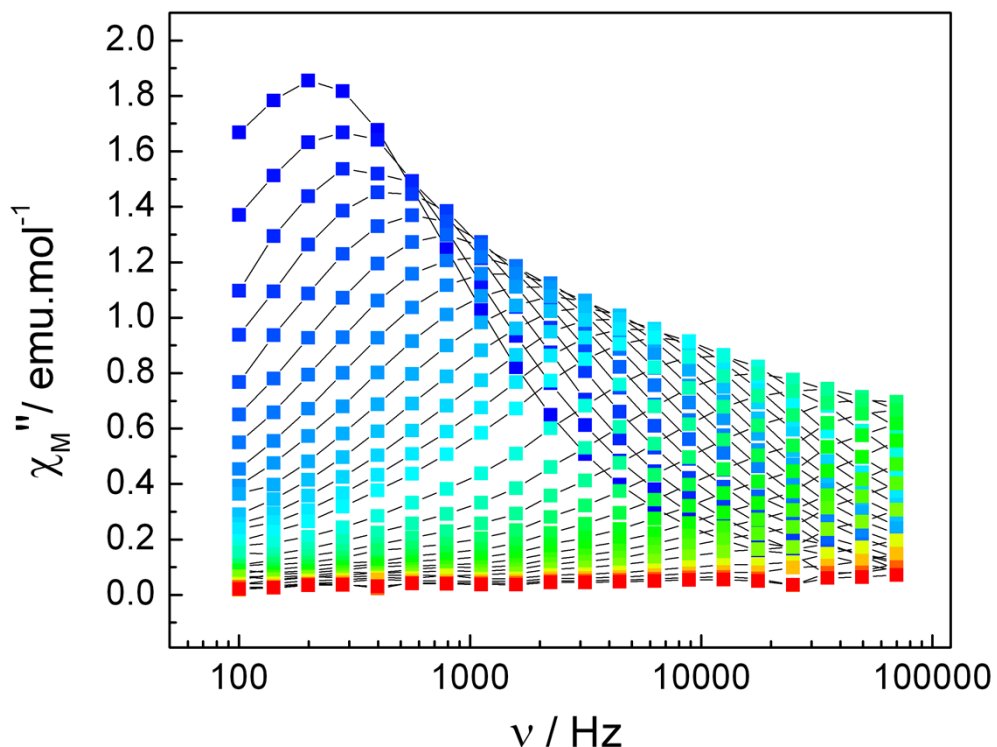


Figure S6. Frequency dependence of the in-phase susceptibility (χ_M'') with temperature ranging from 1.7 (blue) to 7.1 K (red) measured with a 1500 Oe external dc field.

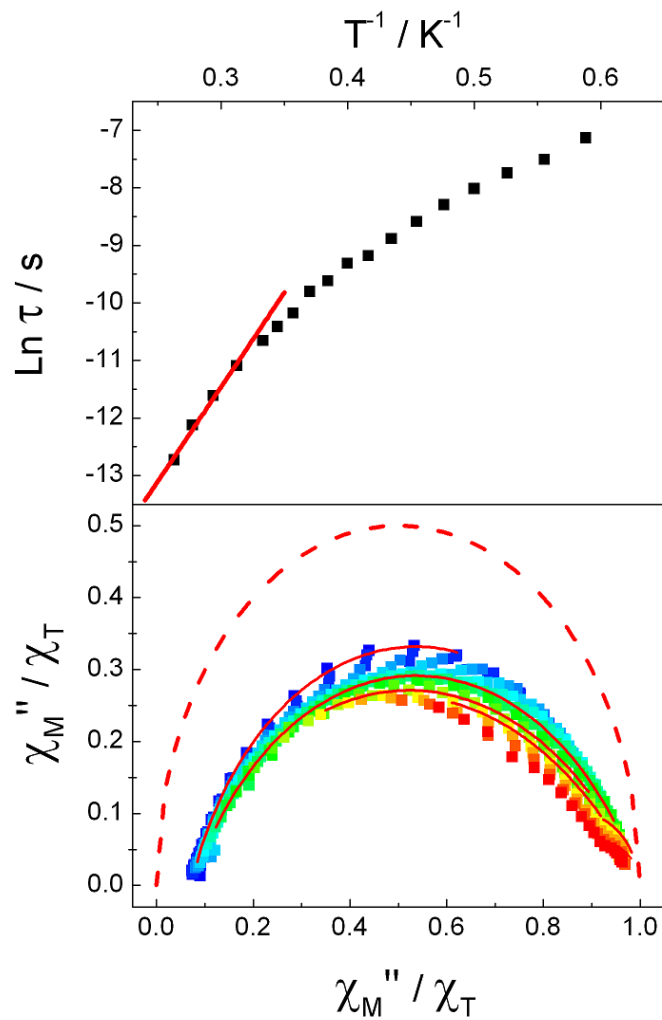


Figure S7. (Top) Arrhenius plot extracted from the in-field measurement of the ac susceptibility with tentative best fit on the highest temperatures. (Bottom) Normalized Argand plot with colour mapping from 1.8 (blue) to 4.2 K (red) with some of the best fits and ideal relaxation curve ($\alpha=0$).

Table S6: extracted values of relaxation rate from the fitting of X'' vs frequency curves

T(K)	τ (μ s)
1.8	547
1.9	432
2	329
2.1	249
2.2	186
2.3	138
2.4	103
2.5	90
2.6	66
2.7	55
2.8	38
2.9	30
3.0	24
3.2	15
3.4	9
3.6	5
3.8	3
4.0	1
4.2	0.8
$\Delta = 33 \pm 2$ K $\tau_0 = 5.5 \times 10^{-10}$ s	

Table S7: extracted values from the fitting of Cole-Cole plots

T (K)	χ_s	χ_T	α	$1 - \chi_s / \chi_T$
1.7	0.333	4.5468	0.21	0.93
1.8	0.594	4.302	0.22	0.86
1.9	0.576	4.14	0.24	0.86
2.0	0.522	4.0428	0.24	0.87
2.1	0.5382	3.8988	0.20	0.86
2.2	0.459	3.798	0.21	0.86
2.3	0.2628	3.627	0.24	0.88
2.4	0.2592	3.5136	0.24	0.93
2.5	0.261	3.4128	0.27	0.93
2.6	0.2286	3.3084	0.28	0.92
2.7	0.2556	3.1554	0.28	0.93
2.8	0.216	2.9808	0.29	0.92
2.9	0.18	2.8278	0.30	0.93
3.0	0.108	2.7018	0.28	0.94
3.2	0.0054	2.592	0.30	0.96
3.4	0.0032	2.4523	0.32	1.00
3.6	0.0010	2.4222	0.34	0.93
3.8	0.0008	2.3800	0.37	0.86

Table S8: calculated charges and potentials

Dy(Murex) ₃ ·11H ₂ O			
	Distance Dy-O (Å)	Charge	Potential* (a.u.)
N _x	2.531	-0.175	-0.037
N _x	2.537	-0.173	-0.036
N _x	2.537	-0.173	-0.036
O _x	2.321	-0.706	-0.161
O _x	2.321	-0.706	-0.161
O _x	2.327	-0.712	-0.162
O _x	2.327	-0.712	-0.162
O _x	2.306	-0.699	-0.160
O _x	2.306	-0.699	-0.160
Dy		2.534	

*Potentials are calculated as q/r , where q is the atomic charge and r the distance between the Dy and the considered atom atoms.

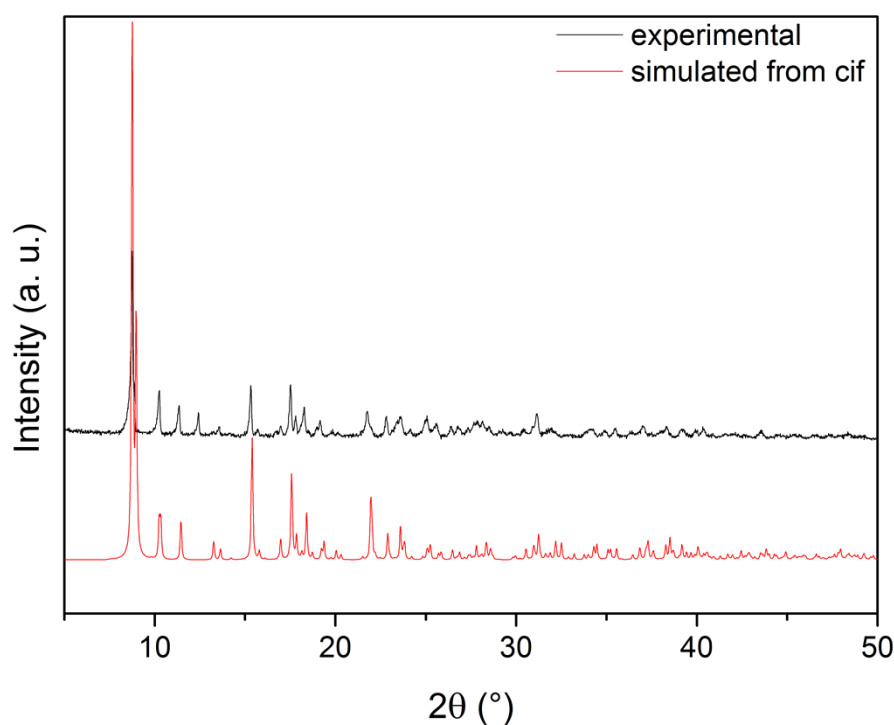


Figure S8. Experimental and simulated X-ray powder diffractograms of **1**.